

PAPER • OPEN ACCESS

Automatic detection of L and T shaped cracks in semifinished casting products

To cite this article: G R Gillich *et al* 2018 *IOP Conf. Ser.: Mater. Sci. Eng.* **393** 012016

View the [article online](#) for updates and enhancements.

You may also like

- [Telephone Circuits](#)
John Perry
- [Analytical and numerical analyses for a penny-shaped crack embedded in an infinite transversely isotropic multi-ferroic composite medium: semi-permeable electro-magnetic boundary condition](#)
R-F Zheng, T-H Wu, X-Y Li et al.
- [Electric and magnetic polarization saturations for a thermally loaded penny-shaped crack in a magneto-electro-thermo-elastic medium](#)
P-D Li, X-Y Li, G-Z Kang et al.



ECS
The
Electrochemical
Society
Advancing solid state &
electrochemical science & technology

DISCOVER
how sustainability
intersects with
electrochemistry & solid
state science research

Automatic detection of L and T shaped cracks in semi-finished casting products

G R Gillich¹, C Tufisi^{1,2}, Z I Korca¹, C O Hamat¹ and N Gillich¹

¹Universitatea “Eftimie Murgu” Resita, P-ta Traian Vuia 1-4, 320085 Resita, Romania

²Spaleck SRL, Str. Castanilor 113, 320022 Resita, Romania

E-mail: gr.gillich@uem.ro

Abstract. The paper presents a method to detect cracks with a complex shape in semi-finished casting products, which bases on the vibration response of the tested element. Firstly, we contrived relative frequency shift curves for beams subjected to L and T shaped cracks by means of the finite element method. The curves were plotted for numerous crack positions along the test specimen and used to contrived crack patterns, which consist of a set of frequency shifts for several weak-axis out-of-plane modes. The patterns are collected in a database and are used as a benchmark in the damage detection process. At the end of the paper, we demonstrate through an experiment how a visual method can be used in an automated damage detection procedure to identify a crack with a complex shape.

1. Introduction

The production of high-quality machine elements implies the use of flawless semi-finished parts which must be, first of all, damage-free. For this aim, the parts to be processed are subject to a quality control. There are several crack detection procedures, which can be grouped into local methods and global methods [1]. Nowadays, global methods are more and more used, due to the benefits they offer: they are quick and allow the detection of all defects at the same time. Among global detection methods, the vibration-based approaches have been proved as simple to be implemented and very reliable [2].

Damages affect the stiffness of the machine element, influencing the vibrational behavior by diminishing the natural frequencies [3]. The stiffness loss and the subsequent frequency drop directly depend on the shape and depth of the crack. Nowadays, a lot of studies are dedicated to cracks assessment [4]-[8]. Despite that, just a few studies took into consideration cracks of a more complex shape, as L or T cracks, because of the degree of difficulty of approaching such cases [9].

From our previous research, we found a function of two variables which can be used to predict natural frequency changes occurring due to transverse cracks with known size and position [10]-[12]. The contrived function, nominated as Relative Frequency Shift (RFS) function, takes into account the square of the modal curvature [13] and the deflection increase due to the crack [14]. By involving this function, one attains similar results to those obtained for cracks modeled as torsional springs without mass. The advantage of employing one function, instead of solving an algebraic system with eight variables for any damage case, is obvious [15]. The RFS function is applicable for beams with any support types, including multiple supports, by simply choosing the proper modal curvature [16]. The variable staying for the damage severity in the RFS function is not influenced by the support types, but only by the depth of the transverse crack [17].



Based on the phenomena described by the RFS function, we succeed to characterize damage signatures by the two crack parameters. The signatures were used to define damage patterns, which are proper to assess damages by employing the inverse method [18]. These patterns were compared with the similar one obtained by involving the finite element method (FEM), and a good fit was remarked [19]. By applying the inverse method supported by the damage patterns, cracks in real structures were successfully assessed [20].

This paper introduces patterns for damages, determined by FEM involvement, which have the form of L or T cracks and have resulted from the longitudinal extension of a transverse crack. The patterns are used for assessment of a crack in a hot-formed flat bar of steel.

2. The development of damage patterns from the Relative Frequency Shift curves

The frequency of a beam decreases from f_U to f_D , in the event of a transverse crack, due to the fact that it loses its stiffness and thus, cannot anymore accumulate the same amount of energy as in the healthy state. The crack depth a determines the damage severity, which is a parameter independent to the crack location; hence it controls the amplitude of the frequency shift curves. On the other hand, the shape of these curves is controlled by the crack location and the vibration mode number. A crack with a given depth differently affects the natural frequency of a vibration mode if it is placed in different beam slices. Regarding the crack with defined depth and position, it differently affects the natural frequencies of different vibration modes.

Examples of frequency evolution curves with respect to the crack location, plotted using FEM simulation results, for the first three vibration modes for a cantilever beam, are illustrated in Figure 1. From here, the RSF for any crack location x and vibration mode i is found as:

$$RFS_i(x) = \frac{f_{iU} - f_{iD}(x)}{f_{iU}} \quad \text{for } x \in [0, L] \quad (1)$$

From Figure 1 clearly results that, for a transverse crack having any position in the beam, we can use the local RSF values of several vibration modes as patterns that characterize the crack location.

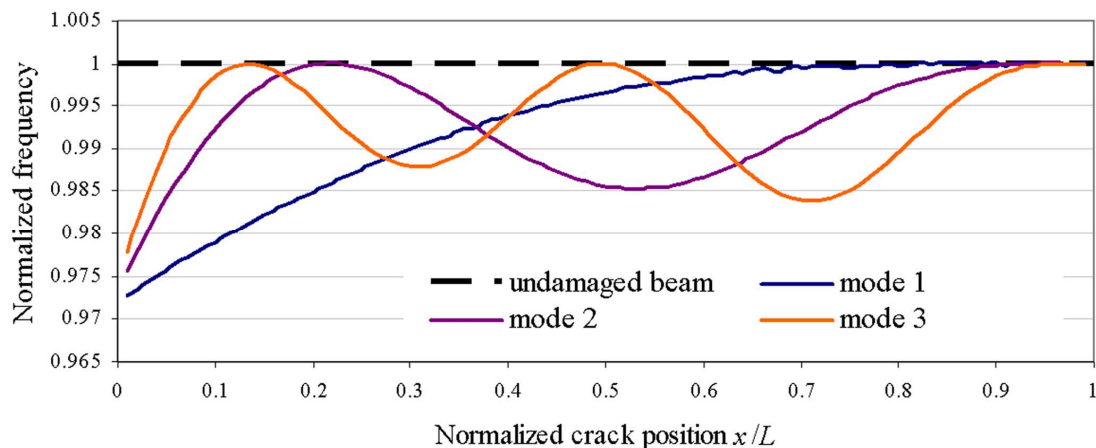


Figure 1. Frequency evolution curves for the first three vibration modes for a cantilever beam.

Figure 2 illustrates the RFS curves for the first six modes of the cantilever beam. Here, the frequency shifts for the normalized crack location $x/L = 0.25$ are highlighted and the resulted values are depicted. If taking the six RFS values for the location $x/L = 0.25$, a histogram as that presented in the left image in Figure 3 is attained. This histogram is, in fact, the damage signature (DS) that corresponds to a damage location $x/L = 0.25$. If one achieves a damage signature by measurements, and compares it to a sequence of RFSs for equidistantly distributed along the beam, one RFS that best fit the DS will be found. The index (x) of this RFS indicates the crack location [13].

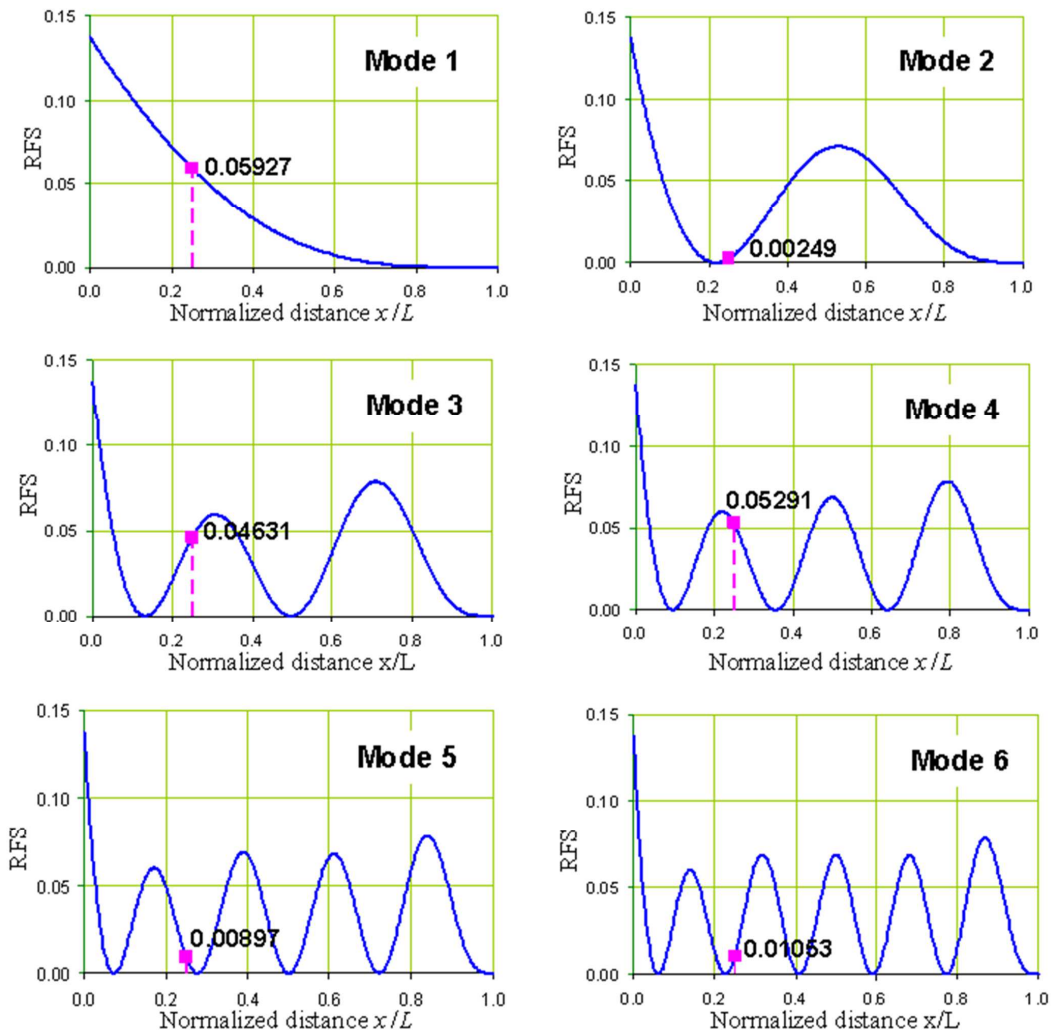


Figure 2. Relative Frequency Shift curves for the first six vibration modes. The RFS values for the crack position $x/L = 0.25$ are highlighted and the values are depicted.

One can construct, by extracting from Figure 2 the RFS values for the crack location $x/L = 0.5$, the histogram shown in the right image of Figure 3. The dissimilarity between the two histograms obtained can be easily observed. In asymmetric structures, each crack location provides a particular DS.

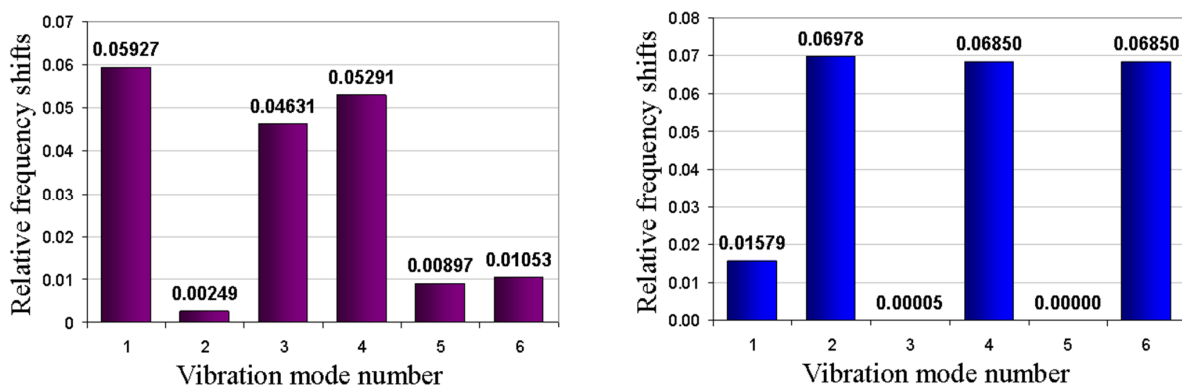


Figure 3. Histograms build for RFS values representing crack locations $x/L = 0.25$ and $x/L = 0.5$.

An algorithm was formulated in order to find the most similar histograms [21]. The algorithm is based on the relation that we derived as a modified Kullback-Leibler Divergence. This relation is:

$$DI_R(x) = \sum_{i=1}^n \log \left| \frac{RFS(x)}{DS} \right|^{-R} \quad (2)$$

and the algorithm consists in finding the crack at the location where the variable x ensures the highest value for DI_R .

$$\text{if } DI_R(x) = \max; \text{ then } x = \text{crack location} \quad (3)$$

This algorithm allows the automation of the damage assessment process. The favorable number of vibration modes to be analyzed is $n = 6 \dots 10$. In the next sections, damage patterns for beams containing L or T shaped crack are derived involving the finite element analysis.

3. Materials and method

The study was performed involving the ANSYS simulation software, by using the modal analysis finite element method (FEM). The current paper considered a prismatic steel beam in healthy state respectively with 4 cracks of different types taken one by one. The beam geometry is described in Table 1, together with the dimensions of the idealized cracks. Figure 4 illustrates the real crack with its idealized representation and the associated parameters.

Table 1. Beam and crack dimensions.

Length L [mm]	Width B [mm]	Thickness H [mm]	Damage case					
			Case	Crack length		Crack depth a [mm]	Crack angle	
				l_L	l_R		α	β
1000	50	5	L _{L50}	50	0	2.5	90	-
			L _{R50}	0	50	2.5	-	90
			T ₅₀	25	25	2.5	90	90
			T ₃₀	15	15	2.5	90	90

The crack position is described by the distance x , which is always considered between the fixed beam end and the transverse crack component, as shown in Figure 4.

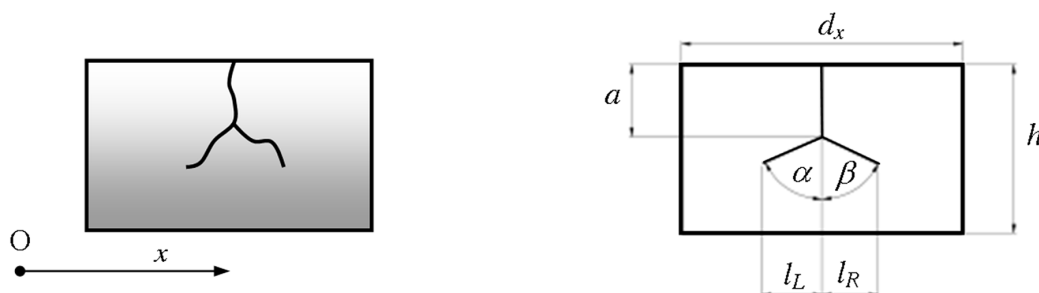


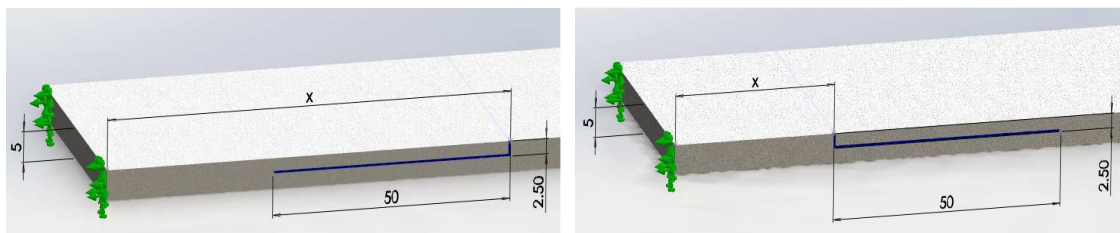
Figure 4. Beam slice of length dx with a complex shaped crack placed at distance x from the left end and its model with idealized edges.

To get a reference, we determined the natural frequencies of the first six bending vibration modes for the undamaged steel beam, which has the physical-mechanical properties presented in Table 2. Afterward, we simulated cracks and performed two types of analysis. The first evaluation focused on the influence of the crack position, while the second one was on the influence of the longitudinal crack extent. For clarity, a detailed description of the cracks involved in the two analyses is given below.

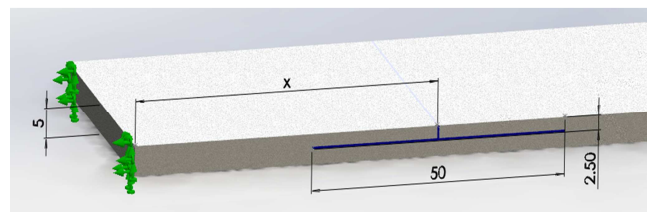
Table 2. Physical-mechanical properties of the steel beam.

Mass density ρ [kg/mm ³]	Young modulus E [N/m ²]	Poisson ratio ν [-]	Tensile strength [MPa]	Yield strength [MPa]	Minimum elongation [%]
7850	$2 \cdot 10^{11}$	0.3	470-630	355	20

The damage case L_{L50} represents an L shaped crack. It has a transverse branch, with depth $a = 2.5$ mm, localized at a distance x from the fixed end. The second crack branch extends to the left side with $l_L = 50$ mm, in the longitudinal direction (see left image in Figure 5). The damage case L_{R50} , depicted in the right image in Figure 5, is similar to the previous case, the difference consisting in the direction of the crack. The damage is extended over $l_R = 50$ mm towards the right side of the transverse crack.

**Figure 5.** Beams subjected to L shaped cracks of type L_{L50} respectively L_{R50} .

The damage cases T_{50} and T_{30} represent cracks with an inverted T shape, located at distance x from the fixed end, having a depth $a = 2.5$ mm and two extensions of length $l_L = l_R$ to the right respectively the left in longitudinal direction. The indexes 50 and 30 indicate the total length $l_L + l_R$ in the longitudinal direction, as illustrated in Figure 6.

**Figure 6.** Beam subjected to a T shaped crack of type T_{50} .

By investigating the effect of the crack position, we took, for both L and T shaped cracks, the left crack end as the reference. We considered the crack end because the longitudinal component is the relevant one. In this way, we assured compatibility of the achieved results. Note that, for the three analyzed damage cases, the longitudinal crack extent is always 50 mm. To find the frequency shifts for a series of crack positions, we derived the natural frequencies of the first six bending vibration modes by iteratively displacing the crack with a step of 10 mm. We started the simulation with the left end of the crack located at 10 mm from the fixed end. It has resulted in a number of 94 studies per case.

The effect of the crack extent was studied by involving the T shaped cracks of length 50 mm and 30 mm, respectively. In this case, we took the position of the transverse crack component as the reference distance from the fixed end. We used the results for the T_{50} damage case earlier derived, with the remark that now the reference distance is associated with the transverse crack position. Similarly, we made simulations to find the frequencies for the T_{30} damage case.

From the obtained results we calculated the RFS and derived the patterns for all four damage cases considering the 94 crack locations per case. This assures a sufficient dense grid, permitting to assess the damage location with a maximal error of 1%. The crack depth can be found from the RFS

corresponding to the crack location if it is compared with a standard RFS calculated for a reference damage depth (lets say 5% of the thickness) for that location.

To test the availability of the contrived patterns, we simulated an L shaped crack by machining the ends of two beams in order to achieve for both of them 50 mm long segments with an eccentric thickness of 2.5 mm, as shown in Figure 7. We superposed the two thinned beam segments and performed a welded seam at the left end of the superior beam, located at $x = 160$ mm from the fixed end. In this way, two faces of the resulted beam are not bounded and an L shaped crack .was achieved.

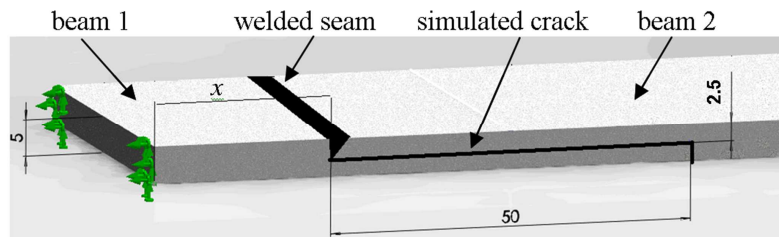


Figure 7. Simulated L_{R50} crack, obtained by welding two beams with machined ends.

The measurements were performed using the experimental stand presented in Figure 8, developed for this purpose. A description of the stand is made in [12], while the frequency estimation algorithm is presented in [20]. Figure 9 illustrates the interface of the VI which implements the algorithm in LabVIEW. The picture shows how the second and the third modes are precisely evaluated.



Figure 8. Experimental stand dedicated for natural frequency estimation of beams.

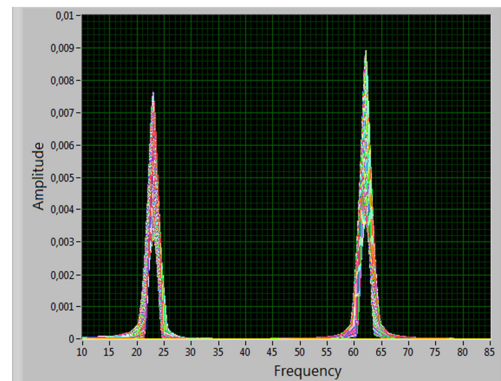


Figure 9. Virtual instrument developed for precise frequency estimation.

We measured the first six natural frequencies of the undamaged beam, which had similar geometry and mechanical parameters as those described at the beginning of this section. Then we measured the homonymous frequencies for the beam with a simulated damage, which we used to calculate the RFSs according to the relation (1). The DS deduced from the RFSs was subjected to the similarity test involving relations (2) and (3). By successfully comparing the DS with all the previously deduced damage patterns, we have proven that the latter are benchmarks that can be used with confidence in the defect detection process.

4. Results and discussion

4.1. Influence of the damage shape on the frequency shifts

To profoundly understand the frequency shift phenomena that occur due to different damage types, we plotted the natural frequency curves for the three types of crack, L_{L50} , L_{R50} and T_{50} . The curves, plotted for the first six weak-axis bending vibration modes, are depicted in Figure 10.

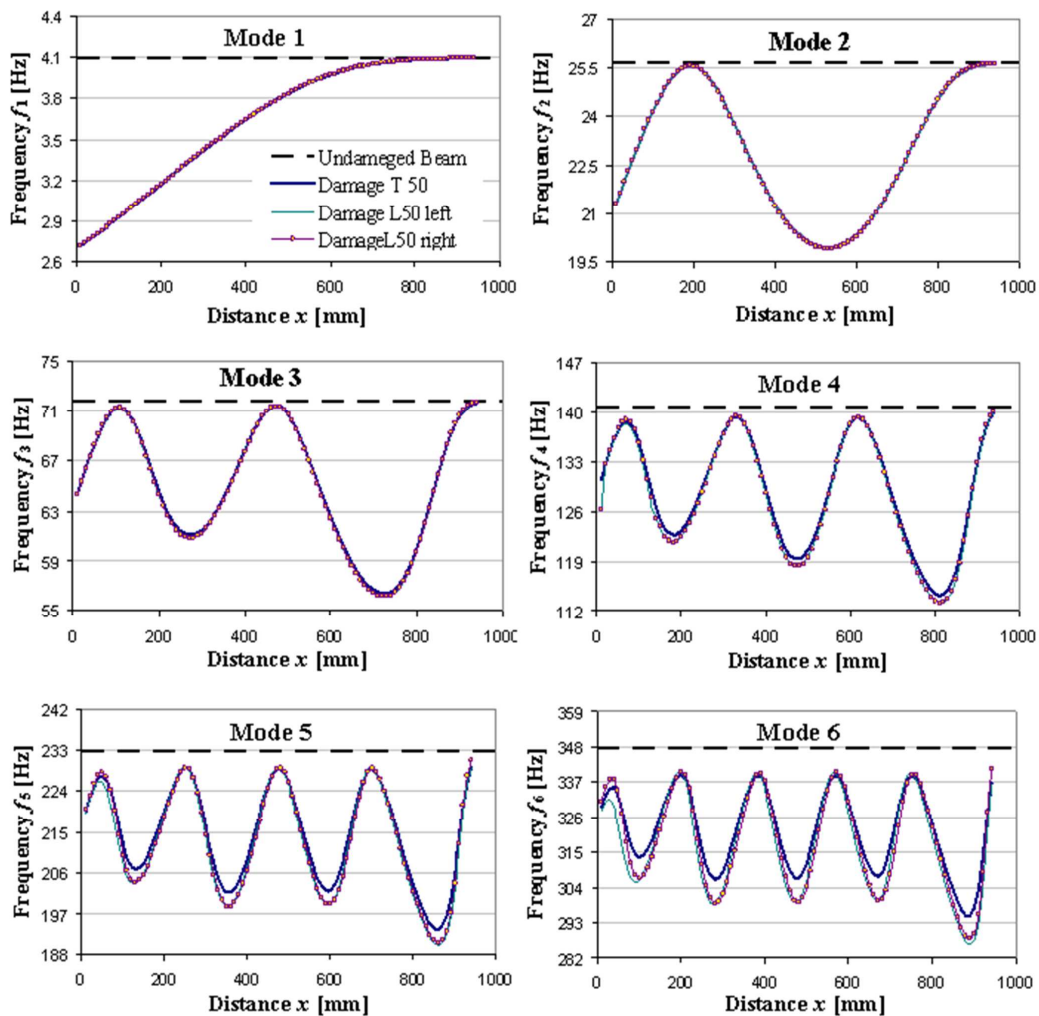


Figure 10. Frequency versus crack location for damages of type L_{L50} , L_{R50} and T_{50} .

From Figure 10 results that the three damages, of type L_{L50} , L_{R50} and T_{50} , considered in this subsection, have a quite similar effect upon the first three vibration modes. Beginning with mode four a behavioral differentiation is observed since the frequency drops for the beam affected by a T_{50} crack are smaller as those of the beams affected by L-type cracks. In addition, near the fixed end, minor differences between frequencies of the beams carrying L_{L50} and L_{R50} cracks are observed.

This finding allow one to conclude that the longitudinal damage branch is relevant to the behavior of a damaged beam, and it should be considered when defining damage patterns for vibration-based nondestructive structural health assessment. The transversal crack branch has the main effect on frequency drop if it is located at one end of the longitudinal crack branch. Intermediate positions of the transversal crack branch lead to lower frequency drops, the lowest drop being obtained if it is situated in the center of the longitudinal crack branch.

As in the case of pure transversal cracks, a sequence of RFS values derived for a specific crack can be used as a pattern in damage assessment. Investigations done by involving the similarity test supported by relation (3) found the best fit between RFSs achieved by measurement and using the FEM for the damage located at a distance $x = 160$ mm, which coincided with the real location.

Table 3 and Figure 11 prove the ability of patterns derived from simulations involving the FEM to indicate the crack position, through the concordance of the results obtained in this way with those attained by measurements.

Table 3. Frequencies and RFS values obtained by simulations for the healthy beam and the beam with LL50, LR50 and T50 damage cases, respectively by measurements on the real beam.

Mode	Frequency [Hz]					RFS		
	FEM simulation			Measurements		L _{L50}	L _{R50}	Real damage
	Healthy beam	L _{L50}	L _{R50}	Healthy beam	Real damage			
1	4.0902	3.0681	3.0686	4.0972	3.1905	0.249853	0.249731	0.221419
2	25.627	25.357	25.365	25.782	25.299	0.010535	0.010223	0.018735
3	71.757	68.312	68.427	72.034	68.332	0.048009	0.046406	0.051384
4	140.631	122.39	122.60	141.219	123.323	0.129708	0.128214	0.126718
5	232.533	208.04	207.45	233.457	210.655	0.105331	0.107868	0.097670
6	347.462	329.15	326.28	348.881	325.214	0.052702	0.060962	0.067835

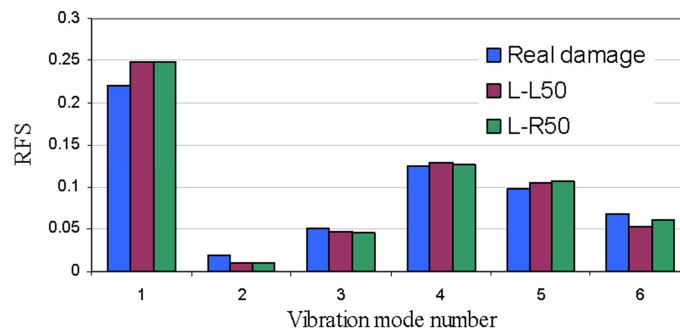


Figure 11. RFS values achieved from measurements for the real damage and from FEM simulations for the cases L_{L50} and L_{R50}.

4.2. Influence of the damage longitudinal extent on the frequency shifts

The evaluation of the damage severity is studied by comparing the effect of two cracks with a T shape, both having the transverse branch with similar depth, but having different dimensions of the longitudinal branches. The way how these cracks, namely T₅₀ and T₃₀, diminish the natural frequencies is illustrated by the natural frequency evolution curves in Figures 12 and 13.

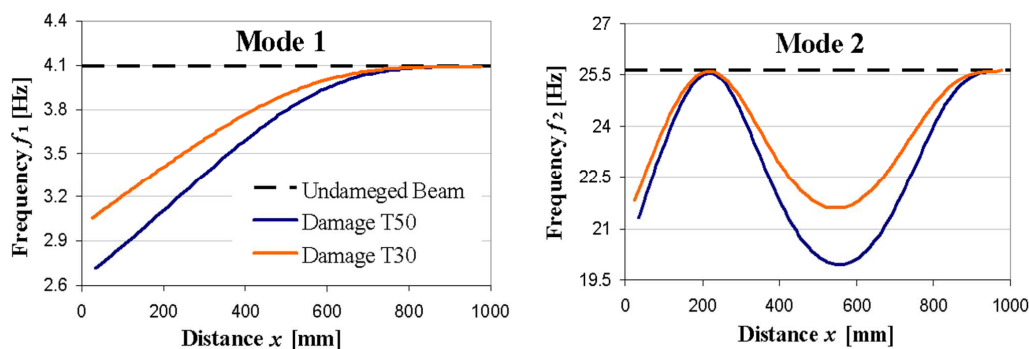


Figure 12. Frequency versus crack location for the beams damaged by T₅₀ and T₃₀ cracks for the first two vibration modes.

From the frequency curves plotted in Figures 12 and 13 it can be concluded that the severity increases with the longitudinal branch extent of the damage, but, apparently, it is not possible to express one severity value for all vibration modes. This issue deserves a deeper analysis in our future studies.

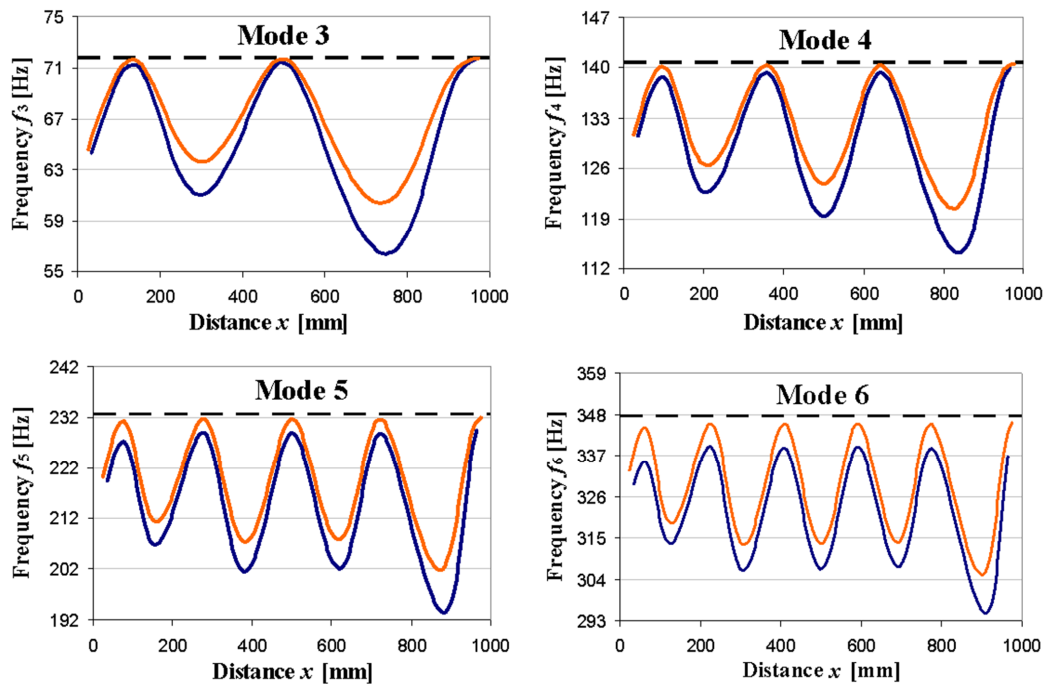


Figure 13. Frequency versus crack location for the beams damaged by T_{50} and T_{30} cracks for the vibration modes four to six.

5. Conclusion

We emerge in this paper how the proposed damage detection method can be used to identify cracks with complex configuration, which may exist in hot-rolled bars. The considered crack configurations were the inverted T and two L shapes that are symmetric to each other around the transversal axis. Frequency evolution curves with defect position were plotted, for all three damage types, using FEM simulation results. From these curves, we found out that the three cracks if having the same length in the longitudinal direction produce similar shifts especially for the first three vibration modes. For the superior modes, the crack with a T shape produces lower frequency drops compared with the L-type cracks. This means that the longitudinal branch of the crack has the relevant effect on the beam dynamics and, therefore, it defines the damage pattern. As a consequence, the position of the longitudinal branch of the crack is rather recognized as the location of its transverse branch. Evaluating the effect of the longitudinal branch length on the T shaped cracks we found the frequency drop is proportional with the length for all damage locations and vibration modes.

The findings confirm that a bi-univocally relation exists between a damage and its signature. On this basis, we succeeded to identify a damage of complex configuration in a hot-rolled bar by involving patterns derived from the RFS curves. It worth mentioning that the bigger the database containing damage pattern is, that higher the precision of assessing damages.

References

- [1] Gillich G R, Birdeanu E D, Gillich N, Amariei D, Iancu V and Jurcau C S 2009 Detection of Damages in Simple Elements, *Annals of DAAAM & proceedings of DAAAM international symposium* **20**(1) 623-625
- [2] Mituletu I C, Gillich N, Nitescu C N and Chioncel C P 2015 A Multi-Resolution Based Method to Precise Identify Thenatural Frequencies of Beams with Application in Damagedetection, *Journal of Physics: Conference Series* **628** 012020
- [3] Gillich G R, Tufoi M, Korca Z I, Stanciu E and Petrica A 2016 The Relations between Deflection, Stored Energy and Natural Frequencies, with Application in Damage Detection,

- Romanian Journal of Acoustics and Vibration* **13**(2) 87-93
- [4] Yang Z B, Radzienski M, Kudela P and Ostachowicz W 2016 Scale-Wavenumber Domain Filtering Method for Curvature Modal Damage Detection, *Composite Structures* **154** 396-404
- [5] Vosoughi A R 2015 A Developed Hybrid Method for Crack Identification of Beams, *Smart Structures and Systems* **16**(3) 401-414
- [6] Mazanoglu A 2015 A Novel Methodology using Simplified Approaches for Identification of Cracks in Beams, *Latin American Journal of Solids and Structures* **12**(13) 2460-2479
- [7] Zhang K and Yan Z 2017 Multi-Cracks Identification Method for Cantilever Beam Structure with Variable Cross-Sections Based on Measured Natural Frequency Changes, *Journal of Sound and Vibration* **387** 53-65
- [8] Khnajar A and Benamar R 2017 A New Model for Beam Crack Detection and Localization using a Discrete Model, *Engineering Structures* **150** 221-230
- [9] Ravi J T, Nidhan S, Muthu N and Maiti S K 2018 Analytical and Experimental Studies on Detection of Longitudinal, L and Inverted T Cracks in Isotropic and Bi-Material Beams Based on Changes in Natural Frequencies, *Mechanical Systems and Signal Processing* **101** 67-96
- [10] Gillich G R and Praisach Z I 2013 Detection and Quantitative Assessment of Damages in Beam Structures using Frequency and Stiffness Changes, *Key Engineering Materials* **569-570** 1013-1020
- [11] Ntakpe J L, Gillich G R, Mituletu I C, Praisach Z I and Gillich N 2016 An Accurate Frequency Estimation Algorithm with Application in Modal Analysis, *Romanian Journal of Acoustics and Vibration* **13**(2) 98-103
- [12] Gillich G R, Praisach Z I and Negru I 2012 Damages Influence on Dynamic Behaviour of Composite Structures Reinforced with Continuous Fibers, *Materiale Plastice* **49**(3) 186-191
- [13] Gillich G R and Praisach Z I 2014 Modal Identification and Damage Detection in Beam-Like Structures using the Power Spectrum and Time-Frequency Analysis, *Signal Processing* **96**(A) 29-44
- [14] Nitescu C, Gillich G R, Wahab M A, Manescu T and Korca Z I 2017 Damage Severity Estimation from the Global Stiffness Decrease, *Journal of Physics: Conference Series* **842** 012034
- [15] Gillich G R, Wahab M A, Praisach Z I and Ntakpe J L 2014 *The Influence of Transversal Crack Geometry on the Frequency Changes of Beams*, International Conference on Noise and Vibration Engineering ISMA, Leuven, Belgium, September 15-17, pp. 485-498
- [16] Ntakpe J L, Praisach Z I, Mituletu I C, Gillich G R and Muntean F 2017 Natural Frequency Changes of Two-Span Beams Due to Transverse Cracks, *Journal of Vibration Engineering and Technologies* **5**(3) 229-238
- [17] Gillich G R, Maia N M M, Mituletu I C, Tufoi M, Iancu V and Korca Z I 2016 A New Approach for Severity Estimation of Transversal Cracks in Multi-Layered Beams, *Latin American Journal of Solids and Structures* **13**(8) 1526-1544
- [18] Gillich G R and Praisach Z I 2012 Damage-Patterns Based Method to Locate Discontinuities in Beams, *Proceedings of SPIE* **8695** 869532-1
- [19] Gillich G R, Praisach Z I, Onchis-Moaca D, Gillich N 2011 *How to Correlate Vibration Measurements with FEM Results to Locate Damages in Beams*, 4th WSEAS International Conference on Finite Differences - Finite Elements - Finite Volumes - Boundary Elements, Paris, France April 28-30, pp **11** 76-81
- [20] Gillich G R, Mituletu I C, Praisach Z I, Negru I and Tufoi M 2017 Method to Enhance the Frequency Readability for Detecting Incipient Structural Damage, *Iranian Journal of Science and Technology, Transactions of Mechanical Engineering* **41**(3) 233-242
- [21] Minda P F, Praisach Z I, Gillich N, Minda A A and Gillich G R 2013 On the Efficiency of Different Dissimilarity Estimators used in Damage Detection, *Romanian Journal of Acoustics and Vibration* **10**(1) 15-18